VARIATIONS IN THE TELECONNECTION INTENSITY INDICES AND THEIR REMOTE RESPONSE TO THE EL NINO EVENTS IN THE NORTHERN HEMISPHERE *

Zhu Qiangen (朱乾根) and *Shi Neng* (施 能)

Nanjing Institute of Meteorology, Nanjing 210044

Received December 29, 1991

ABSTRACT

In this study, the monthly and seasonal teleconnection intensity indices of the Pacific / North American (PNA), Western Atlantic (WA), Western Pacific (WP), Eastern Atlantic (EA) and Eurasian (EU) patterns for the period from 1951 through 1990 are calculated. On this basis, their climatic variations and the relationship between the five teleconnection intensity indices and the El Nino events are examined. It is noted that when El Nino is at its mature stage (winter), the weak WP pattern is mainly characteristic of the circulation and the strong PNA pattern is the next. In summer when El Nino occurs and develops, the strong EU, weak WP and weak WA patterns are the main characteristics without the PNA circulation anomalies. Finally, by the nonlinear mapping method a nonlinear mapping diagram is established for diagnosing El Nino using three summer teleconnection intensity indices and May and August Southern Oscillation Indices (SOIs). Thus, the El Nino phenomenon occurring in 1991 is diagnosed. Besides, the winter atmospheric circulation of the 1991 / 1992 El Nino is found to be the weak WP pattern and the PNA pattern is also weak.

Key words: teleconnection pattern, El Nino, nonlinear mapping, remote response

I. INTRODUCTION

Wallace and Gutzler (WG for short) (1981) put forward five northern teleconnection patterns from years of observational study in the northern winter, namely, the PNA, WA, WP, EA and EU patterns. Study of these patterns will contribute to the understanding of the quasi–stationary structure of the northern winter atmospheric circulation and the improvement of long– and short–range weather forecasting.

Recently meteorologists have made many investigations on the El Nino events and the air–sea interaction. It seems that the concept of teleconnection is related to the following views: in the ENSO events the remote response of the northern winter to the equatorial heat source causes stationary waves corresponding to the baratropic structure, producing the PNA pattern. Shukla and Wallace (1983), Hoskins and Karoly (1981), and Huang (1986), using numerical models, pointed out that the sea surface temperature (SST) anomaly in the equatorial east Pacific would cause the PNA atmospheric circulation anomaly in the Northern Hemisphere.

However, it is important to note that while putting forward the five teleconnection patterns, WG only calculated teleconnection indices of 15 winters, i.e., the wintertime from

* This study is sponsored by the National Natural Science Foundation and Monsoon Research Funds.

1962 / 1963 to 1976 / 1977. The El Nino events occurring during this period of time are less than half of the events in 40 years. As lots of literature have mentioned, the PNA pattern causing the 1976 / 1977 severe winter in North America was the strongest PNA pattern in this time period. According to the calculation in this study, the 1976 / 1977 winter has experienced the strongest PNA pattern in the past 40 years. In fact, there has not been much similarity in the geographic distribution of temperature over the United States in the El Nino winter for the last 40 years. Recently, Huang (1991) pointed out the absence of the PNA pattern in the El Nino winter of 1972 / 1973 and the role that the basic flow plays in the propagation of the planetary waves. Moreover, when the strong PNA pattern is observed in winter, the El Nino does not necessarily occur. Even when the anti–PNA pattern (the PNA intensity is negative) is experienced in winter, the El Nino phenomenon is probably occurring. So far observational studies have not yielded perfect results. Besides, numerical modelling has not been very encouraging. In terms of the model of Goddard Laboratory for Atmospheric Sciences (GLAS) for time integration, Shukla and Wallace (1983) has simulated, from the composite El Nino SST anomaly, the response which is very similar to the actual El Nino circulation. However, Fennessy et al. (1985) could hardly simulate the 1982 / 1983 winter circulation anomaly by using a similar model. Then just what is the relationship between the teleconnection pattern and the El Nino event? Which of the El Nino winters correspond to the PNA pattern and which do not? Which of the teleconnection patterns are abnormal? And it is necessary to make detailed study of the characteristics of the teleconnection patterns during the occurrence and development of El Nino in addition to the circulation patterns when El Nino is at its mature stage. All these observational studies are of significance to the thorough investigation of the El Nino phenomena and the air–sea interaction and to the theory of numerical models and their application.

In this study, the time period for the teleconnection intensity indices defined by WG is first increased from 15 to 40 years and expanded from winter to four seasons (twelve months). Section II gives the calculation results and discusses their reliability and accuracy. In Section III their intermonthly variations and lag correlation characteristics are examined. Section IV shows the teleconnection patterns when El Nino is at its mature stage. The characteristics of the circulation anomalies during the El Nino occurrence and development are given in Section V, in which the nonlinear mapping diagram showing the diagnosis of El Nino by using the pre–August teleconnection intensity indices and the SOI is established. The conclusion is presented in Section VI.

II. THE NORTHERN TELECONNECTION PATTERNS AND THEIR INTENSITY INDICES

Fig. 1 gives the northern teleconnection patterns defined by WG. And the geographic locations of the atmospheric activity centers are shown in Table 1.

From the height values at the 500 hPa of the atmospheric activity centers and by standardization, the Jan. 1951— Dec. 1990 monthly teleconnection intensity indices of the five teleconnection patterns are calculated. The 500 hPa height data come from the long–range weather prediction data bank tapes of the State Meteorological Administration and the calculations are all completed on the M–360 computer. The seasonal teleconnection mean intensity indices are thus determined from the monthly data, spring (March— May), summer (June—Aug.), autumn (Sep.—Nov.) and winter (Dec.—Feb.). For the limit of space, only the winter teleconnection pattern indices are given in Table 2.

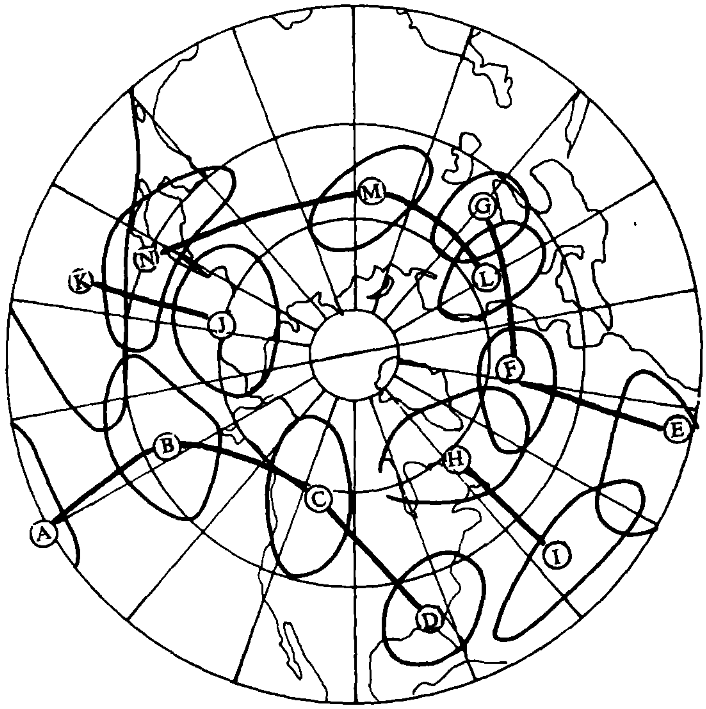

Fig. 1. The teleconnection patterns defined by Wallace and Gutzler (1981) and the corresponding atmospheric activity centers (meaning of A–N see Table 1).

Table 1. The Teleconnection Patterns and Their Activity Centers

Sequence	Geographic location	Pattern
A	20°N, 160°W	PNA
B	45°N, 165°W	
C	55°N, 115°W	
D	30°N, 85°W	
E	25°N, 25°W	EA
F	55°N, 20°W	
G	50°N, 40°E	
H	55°N, 55°W	WA
I	30°N, 55°W	
J	60°N, 155°E	WP
K	30°N, 155°E	
L	55°N, 20°E	EU
M	55°N, 75°E	
N	40°N, 145°E	

What is the reliability of the data given in Table 2 ? WG has made calculations for the winter period of 1962 / 1963—1976 / 1977. It is necessary to compare WG's results with those given for the 40–year period in Table 2. Strictly speaking, it is desirable to examine the frequency

Table 2. The Winter Intensity Indices of the Northern Teleconnection Patterns (1951 / 1952—1991 / 1992)

Year	PNA	WA	WP	EA	EU
1951	−0.84	−0.22	−0.49	0.17	0.49
1952	0.33	0.46	0.05	0.88	0.28
1953	−0.33	−0.42	−0.33	0.40	−0.81
1954	−0.61	1.12	0.18	0.19	0.40
1955	−0.97	0.55	0.98	0.55	−0.05
1956	−1.15	−0.79	1.01	−0.40	−0.15
1957	0.79	1.40	−0.37	0.14	0.16
1958	−0.17	−0.61	−0.46	−0.16	−0.14
1959	0.55	0.57	−0.47	−0.84	−0.01
1960	0.64	−0.98	0.05	−1.29	0.11
1961	−0.31	−0.45	0.95	−0.24	0.64
1962	0.38	−0.02	1.23	0.57	0.73
1963	0.72	−0.23	−0.51	0.57	−0.56
1964	−0.71	0.66	0.32	0.72	0.30
1965	−0.21	0.56	−1.04	−0.99	0.15
1966	0.06	−0.05	−0.41	0.15	0.41
1967	−0.10	1.08	0.97	0.94	0.82
1968	−0.59	1.14	−0.60	−0.04	−1.04
1969	0.66	0.72	−0.24	−0.13	0.49
1970	−0.56	−0.01	0.48	0.21	−0.53
1971	−1.20	−0.52	−0.40	0.07	−1.35
1972	0.09	−0.42	−0.83	−0.30	−1.06
1973	−0.26	−0.25	0.77	−0.50	0.00
1974	−0.11	−0.34	−0.10	−0.07	0.12
1975	−0.12	−0.06	−0.00	1.01	−0.28
1976	1.21	0.03	−0.13	−0.68	0.56
1977	0.81	0.22	−0.16	−0.26	−0.12
1978	−0.48	0.32	−0.94	−0.25	−0.56
1979	0.34	0.12	0.13	−0.17	0.01
1980	0.76	0.24	0.95	0.32	0.73
1981	−0.56	0.10	−0.06	−0.36	−0.04
1982	0.94	0.09	−0.84	0.19	0.10
1983	0.22	−0.53	0.99	−0.54	0.72
1984	−0.29	−0.21	0.39	0.35	0.26
1985	0.88	−0.75	0.55	−0.10	0.65
1986	0.86	0.66	−0.35	0.29	−0.21
1987	0.33	−0.43	−0.99	−0.17	0.06
1988	−0.66	−0.93	−0.85	0.40	−0.91
1989	−0.21	−1.04	−0.33	−0.77	−0.19
1990	−0.11	−0.80	0.92	0.10	−0.19

distribution to see whether there is difference between the two series. But this would be too complicated. We have calculated the correlation coefficients by taking 15 years and 45 months respectively as the sequence lengths, with the results shown in Table 3.

It is seen from Table 3 that they are closely related and their interannual tendencies are in complete agreement. Besides, the correlation matrixes are calculated for the teleconnection intensity indices in this time period and very little difference is observed as shown in Table 4.

Table 3. Comparison between WG's Results and Those in Table 2 (1962 / 1963—1976 / 1977 Winters)

Pattern	PNA	WA	WP	EA	EU	Sequence length
Seasonal data	0.96	0.95	0.89	0.98	0.99	15 years
Winter month data	0.92	0.92	0.92	0.95	0.96	45 months

Table 4. Comparison between WG's Results with Those in Table 2 (Correlation Matrixes of the Pattern Intensity Indices) (1962 / 1963—1976 / 1977 Winters)

	WG's				In this study			
	PNA	WA	WP	EU	PNA	WA	WP	EU
EA	−0.01	0.39	0.04	0.24	−0.05	0.36	0.10	0.28
PNA		0.18	0.07	0.42		0.18	0.00	0.41
WA			−0.07	0.38			−0.08	0.36
WP				0.22				0.30

It seems that these slight errors are totally due to the difference in the length of the calculation periods. As the 500 hPa values of the atmospheric activity centers in the teleconnection intensity index calculation equations must be standardized, WG did the calculation using the mean values and mean square deviations of 15 years, while we calculate the yearly intensity indices indices using those of 40 years (1951—1990).

III. SOME CLIMATIC CHARACTERISTICS OF THE TELECONNECTION PATTERN INTENSITY INDICES

1. *Intermonthly (Interseasonal) Variation of Mean Square Deviations*

Tables 5 and 6 show the mean square deviations of the monthly and seasonal teleconnection patterns respectively.

Table 5. Mean Square Deviations of the Monthly Teleconnection Intensity Indices (1951—1990)

Pattern	M	A	M	J	J	A	S	O	N	D	J	F
PNA	0.79	0.68	0.60	0.51	0.49°	0.51	0.68	0.65	0.71	0.78	0.83*	0.83*
WA	0.90*	0.76	0.77	0.81	0.65°	0.76	0.68	0.78	0.77	0.88	0.81	0.88
WP	0.84	0.82	0.88	0.81	0.70	0.69	0.66°	0.72	0.79	0.92*	0.87	0.87
EA	0.66	0.74	0.61	0.60°	0.67	0.69	0.63	0.69	0.75	0.76	0.79*	0.78
EU	0.74	0.71	0.65	0.64	0.66	0.59°	0.69	0.74	0.67	0.75	0.86*	0.79

Note: Superscripts " * " and " o" denote maximum and minimum values, respectively.

As the indices are the linear composition of standardized variables, the monthly and seasonal means are all zero. It is seen from Tables 5 and 6:

(1) As regards the monthly intensity indices, the PNA pattern occured in January—February, the WA pattern in March, the WP pattern in December, the EA pattern in January, and the EU pattern in January, all with the maximum mean square deviation. This indicates that there is significant interannual variation in the strongest and weakest teleconnection patterns (the maximum negative index) in these months. In contrast, the PNA and WA patterns have their

minimum mean aquare deviations in July, the WP pattern in September, the EA pattern in June and the EU pattern in August, indicating the weak intensity and small annual variation of the teleconnection patterns in these months.

(2) As regards the seasonal intensity indices, the five teleconnection patterns all have their maximum mean square deviations in winter, but their minima appear in different seasons. The PNA and EU patterns have their minima in summer, the WA and WP patterns in autumn and the EA pattern in spring.

Table 6. Mean Square Deviations of the Seasonal Teleconnection Pattern Intensity Indices (1951—1990)

Pattern	Spring	Summer	Autumn	Winter
PNA	0.51	0.35^{o}	0.47	0.63^{*}
WA	0.47	0.53	0.46^{o}	0.61^{*}
WP	0.52	0.43	0.38^{o}	0.64^{*}
EA	0.37^{o}	0.48	0.47	0.52^{*}
EU	0.42	0.37^{o}	0.43	0.54^{*}

Note: Superscripts " * " and " o" denote maximum and minimum values, respectively.

2. *Lag Autocorrelations of the Seasonal and Monthly Teleconnection Intensity Indices*

Table 7 gives the lag autocorrelation coefficients of the five teleconnection patterns with their beginning months in different seasons.

Table 7. Seasonal Lag Autocorrelation Coefficients

Beginning season	Spring				Summer				Autumn				Winter			
Number of season lagging	1	2	3	4	1	2	3	4	1	2	3	4	1	2	3	4
PNA	0.34^{*}	0.21	0.08	0.28	0.00	−0.02	0.11	0.33^{*}	0.39^{*}	0.16	0.11	0.08	0.34^{*}	0.23	0.03	0.04
WA	0.16	0.05	0.06	−0.04	0.14	0.15	0.01	0.46^{*}	0.12	0.04	0.23	0.40^{*}	0.21	−0.27	0.09	0.10
WP	0.01	0.03	−0.30	−0.12	0.41^{*}	0.09	0.31^{*}	−0.13	-0.32^{*}	0.05	0.12	0.22	−0.03	0.09	0.05	0.06
EA	0.24	0.24	0.30	0.14	0.22	0.13	0.38^{*}	0.36^{*}	0.02	0.09	0.09	0.34^{*}	0.24	0.08	0.14	0.03
EU	0.26	0.07	0.16	−0.08	0.20	0.25	0.00	0.26	−0.20	−0.20	0.03	−0.07	0.21	0.15	0.02	0.06

Note: Confidence more than 0.05 is marked by * .

(1) *Characteristics of the seasonal lag autocorrelation*

It is seen from Table 7:

(1) With one–season lag, the PNA pattern intensity index has strong autocorrelation in spring, autumn and winter. The WP pattern intensity index in summer and autumn also has strong autocorrelation of one–month lag, but its autumn autocorrelation of one–month lag is −0.32. That is, the strong summer WP pattern is followed by the strong autumn WP, but in winter it becomes the weak WP pattern, and vice versa.

(2) With two–season lag, none of the patterns show pronounced autocorrelation.

(3) With three–month lag, only the summer WP and EA patterns show lag autocorrelation.

(4) Both the WA and EA pattern intensity indices have significant one–year (four–seasons) lag autocorrelation characteristics in summer and autumn.

(5) The EU teleconnection pattern seasonal intensityy index has no significant lag autocorrelation characteristics.

The above observation and calculation results are of much significance to the recognition of the laws governing the atmospheric circulation variations. However, their physical mechanisms remain to be further studied.

(2) *Characteristics of the monthly lag autocorrelation*

While calculating the monthly lag autocorrelation, we use every month instead of the beginning month. For eliminating the slight fluctuation in the annual variation, weighted running averaging is made of the correlation coefficients calculated. For example, R_{5-6} represents the autocorrelation coefficient of one–month lag with May as the beginning month, the final running correlation coefficient is

$$R'_{5-6}=\frac{1}{4}(R_{4-5}+2R_{5-6}+R_{6-7}),$$

where R_{4-5} and R_{6-7} are autocorrelation coefficients of one–month lag with April and June as the beginning month respectively. All the calculations have been treated this way and their results are shown in Fig. 2, in which the blackened areas indicate confidence more than 0.05, the hatched areas the isolines of 0.20 with their intervals being 0.10, and the broken–line areas are negatively correlative.

It is seen from Fig. 2:

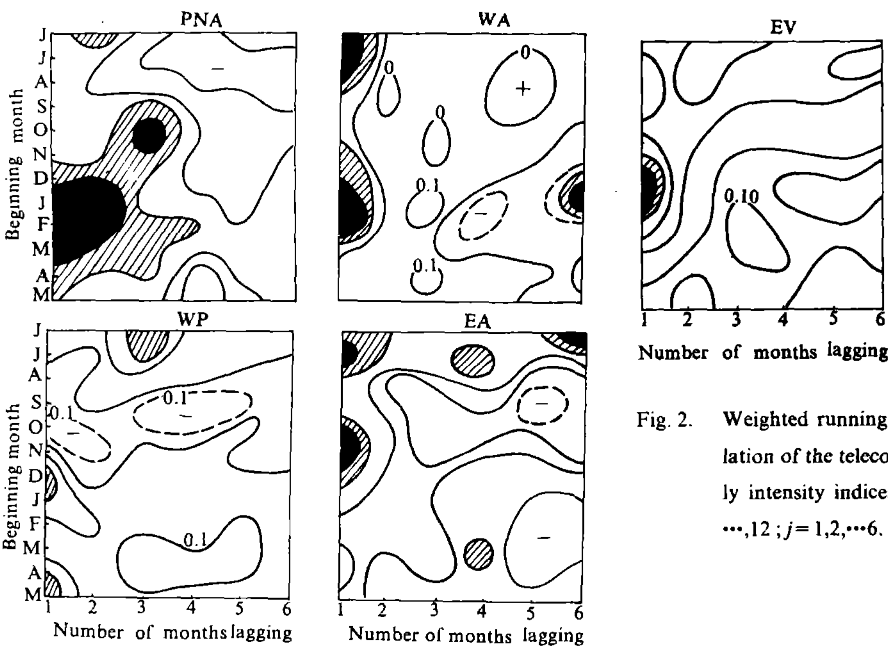

Fig. 2. Weighted running mean lag correlation of the teleconnection monthly intensity indices (R'_{i-j}). $i=1,2,\cdots,12$; $j=1,2,\cdots6$.

(1) In Dec.—March, the PNA pattern monthly intensity index shows good persistence, with autocorrelation coefficient of two–month lag still exceeding confidence of 0.05.

(2) Both the WP and EU pattern monthly indices show weak persistence, with correlation coefficient of one–month lag reaching confidence of 0.05 only in December.

(3) In summer months the WA and EA patterns have weak persistence and show bimodal characteristics. The WA pattern shows good persistence in winter months and the EA pattern in Oct.—Dec., with correlation coefficient of one–month lag reaching confidence of 0.05 only in one month.

IV. ATMOSPHERIC CIRCULATION ANOMALIES WHEN EL NINO IS AT ITS MATURE STAGE

In general, in winter when El Nino is vigorous the atmospheric circulation anomaly assumes the PNA pattern in the Pacific and North America. Many numerical simulations show that the heat source anomaly in the low–latitude east Pacific will increase the PNA circulation anomaly. Normally, the result is basically true. However, this is not necessarily the case in certain El Nino years. For example, when the 1972 / 1973 El Nino developed to its mature stage, the Northern Hemisphere did not experience the strong PNA pattern. Generally, in the El Nino winter the air temperature in the northern part of Northeast China a severe winter is often observed. But in 1972—1973 the area experienced a warm winter (Huang, 1991). Thus, it is necessary to make a study of the different anomalous circulation patterns probably occurring when El Nino is at its mature stage. By using 40 yeras of intensity indices of the five teleconnection patterns, we have tested the difference significance between the El Nino and anti–El Nino years and calculated the statistic of t

$$t = \frac{\bar{x}_1 - \bar{x}_2}{\sqrt{\dfrac{n_1\sigma_1^2 + n_2\sigma_2^2}{n_1 + n_2 - 2}}\sqrt{\dfrac{1}{n_1} + \dfrac{1}{n_2}}},$$

where $\bar{x}_1$, σ_1, and $\bar{x}_2$, σ_2, are the mean values and mean square deviations for the intensity indices of the teleconnection patterns calculated in the El Nino and anti–El Nino years respectively, and n_1 and n_2 are the numbers of El Nino and anti–El Nino years respectively ($n_1 = 10$, $n_2 = 7$). Table 8 gives the calculation results.

It is seen from Table 8:

(1) In the El Nino winter, the WP pattern shows pronounced anomaly, with confidence reaching 0.001, the PNA pattern is the next, with confidence being 0.01 and then the EA pattern, 0.05. As regards the WA and EU patterns, the difference is not significant. Significance tests for the difference between the teleconnection intensity in the El Nino years shown in Table 7 and the secular (40 years) teleconnection intensity gives the same conclusion.

(2) As shown in Table 8, the WP indices are all negative (less than −0.13) in the El Nino years and all positive in the anti–El Nino years. Therefore, it seems that the atmospheric circulation is bound to have the characteristics of the weak WP pattern when El Nino is vigorous. However, it can not be assumed that the strong PNA pattern invariably exists in winter. In fact, in the El Nino years of 1972, 1965, 1953, and 1951, the weak PNA or anti–PNA pattern rather than the strong PNA occurred. It should be noted that Quinn et al. (1978) classified the year of 1972 as the strong El Nino year, 1965 and 1953 as the moderate ones, and 1963 and 1969 as the

weak ones. Therefore, the relationship between the heating field of the equatorial east Pacific SST and the PNA pattern is not a simple linear one. Both theoretical explanation and numerical simulation remain to be further examined.

Fig.3 is the scatter diagram showing the PNA and WP intensity indices (winter) with El Nino and anti–El Nino. In Fig.3 the 40 data spots scatter in the four quadrants, indicating that the two indices are basically independent. However, the anti–El Nino years gather in the second quadrant, the El Nino years scatter in the third and fourth quadrants, and the demarcation line (dashed line) is on the whole parallel to the transversal axis, indicating once again that in the El Nino winter the atmospheric circulation anomaly is basically characteristic of the weak WP pattern and then of the strong PNA pattern. According to the definition of the teleconnection pattern, such a circulation is characterized by the negative anomaly over the Aleutian area, i.e., the Aleutian low becomes deepened, the subtropical high intensified, the high in northwestern Canada enhanced and the trough in central and eastern America deepened, with the characteristics of the deepening of the Aleutian low and the strengthening of the subtropical high more pronounced (the weak WP pattern).

Table 8. Winter Teleconnection Intensity Indices and Their Statisitc t in the El Nino and Anti–El Nino Years

		WP	PNA	EA	WA	EU
El Nino	1951 / 1952	−0.49	−0.84	0.17	−0.22	0.49
	1953 / 1954	−0.33	−0.33	0.40	−0.42	−0.81
	1957 / 1958	−0.37	0.79	0.14	1.40	0.16
	1963 / 1964	−0.51	0.72	0.57	−0.23	−0.56
	1965 / 1966	−1.04	−0.21	−0.99	0.56	0.15
	1969 / 1970	−0.24	0.66	−0.13	0.72	0.49
	1972 / 1973	−0.83	0.09	−0.30	−0.42	−1.06
	1976 / 1977	−0.13	1.21	−0.68	0.03	0.56
	1982 / 1983	−0.84	0.94	0.19	0.09	0.10
	1986 / 1987	−0.35	0.86	0.29	0.66	−0.21
	Mean value	−0.513	0.389	−0.034	0.217	−0.069
	Mean square deviation	0.281	0.634	0.468	0.567	0.542
Anti-El Nino	1954 / 1955	0.18	−0.61	0.19	1.12	0.40
	1955 / 1956	0.98	−0.97	0.55	0.55	−0.05
	1964 / 1965	0.32	−0.71	0.72	0.66	0.30
	1967 / 1968	0.97	−0.10	0.94	1.08	0.82
	1970 / 1971	0.48	−0.56	0.21	−0.01	−0.53
	1973 / 1974	0.77	−0.26	−0.50	−0.25	0.00
	1975 / 1976	0.00	−0.12	1.01	−0.06	−0.28
	Mean value	0.529	−0.476	0.446	0.441	0.094
	Mean square deviation	0.359	0.302	0.488	0.516	0.418
	$\|t\|$	6.296	3.149	1.921	0.781	0.628

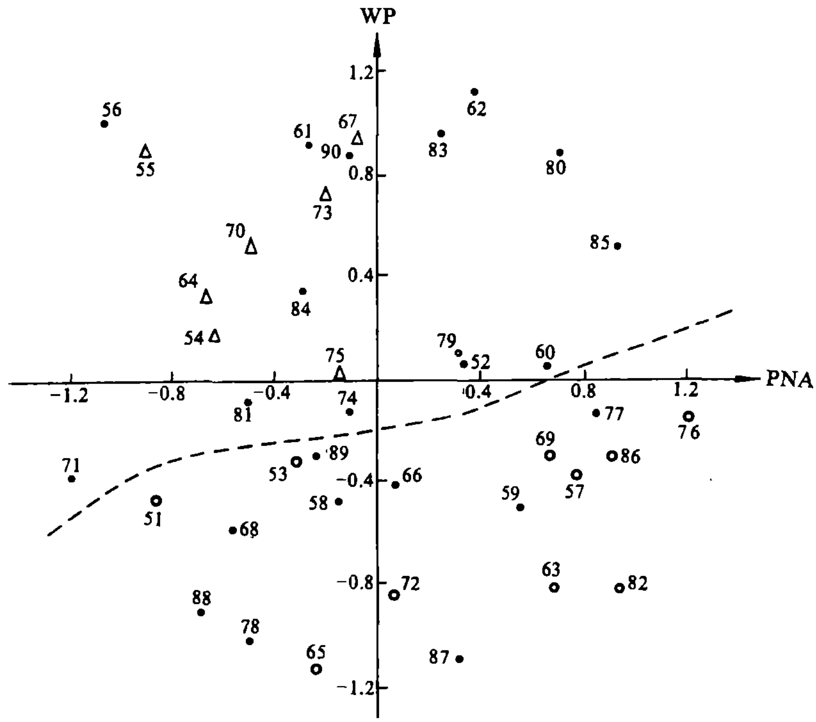

Fig. 3. The winter PNA and WP intensity indices with El Nino and anti–El Nino (1951 / 1952—1990 / 1991). The big circle indicates El Nino, the triangle anti–El Nino and the small black dot the normal year.

Table 8 also shows that generally in the El Nino year the pattern is the weak EA and in the anti–El Nino year the strong EA. It is noteworthy that in 1991 there occurred a new El Nino event. In the equatorial eastern Pacific the SST increased and the SOI had been negative for 12 months running since March, 1991. What characteristics will the winter circulation have this year? Our calculation shows that PNA = –0.23 and WP = –0.59 in the 1991 / 1992 winter. Then a weak rather than a strong PNA occurred in the El Nino event and the weak WP circulation anomaly was observed (see Fig. 3).

V. CHARACTERISTICS OF THE ATMOSPHERIC CIRCULATION DURING THE EL NINO OCCURRENCE AND DEVELOPMENT AND THE STATISTICAL DIAGNOSIS OF EL NINO

Hoskins (1981) has pointed out that the response of the atmosphere to thermal forcing

Table 9. Mean Values and Statistics t of the Summer Teleconnection Coefficients in the El Nino and Anti–El Nino Years

Teleconnection pattern	EU	WP	WA	EA	PNA
Mean value in the El Nino year $n=10$	0.11	–0.19	–0.127	–0.01	–0.038
Mean value in the anti–El Nino year $n=7$	–0.32	0.27	0.336	0.13	–0.059
Mean difference	–0.43	–0.46	–0.463	–0.14	0.021
$\|t\|$	1.96	1.64	1.71	1.34	0.128
Characteristic in the El Nino year	strong	weak	weak	weak	—

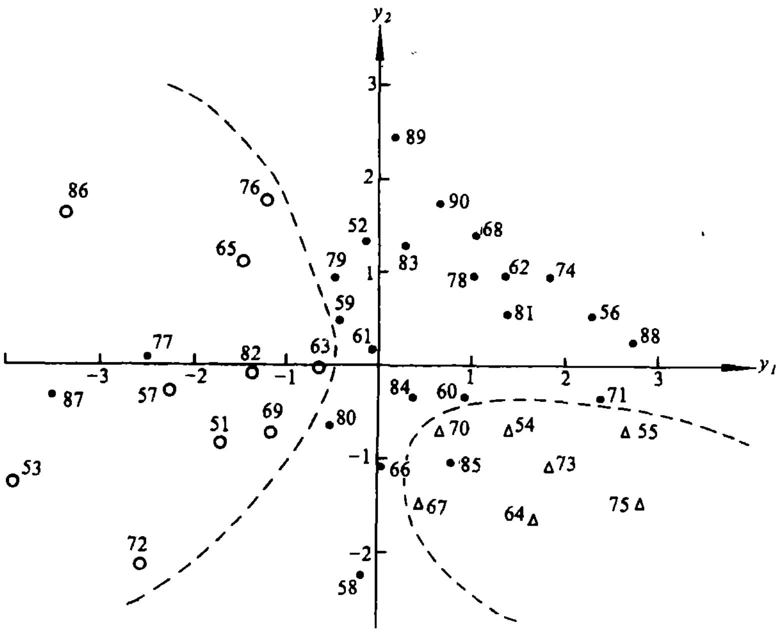

Fig. 4. The two–dimensional mapping of dianosing El Nino and anti–El Nino by using teleconnection intensity indices and SOIs.

has time scale of only several days to several weeks. Then we have calculated the summer intensity index statistics t of the five teleconnection patterns with the results shown in Table 9.

In the summer of the El Nino year the teleconnection pattern is usually the strong one, i.e., along the high and middle latitudes from Europe to East Asia the 500 hPa planetary waves show remarkable characteristic features: the trough is situated near 30°E, a little west of its normal location, the Siberian anticyclone is rather powerful, and in Japan and most part of China the summer air temperature shows negative anomalies while the WP and WA patterns are weak, indicating that the Aleutian low becomes deepened, the subtropical high strengthened, the Icelandic low also deepened and the western Atlantic jet rather strong. However, generally when El Nino occurs and develops the atmospheric circulation anomaly is not so pronounced as when El Nino is at its mature stage.

It is hoped at present that El Nino occurrence can be forecasted by long–range prediction. Although there are many real–time monitoring means available now it has been difficult to predict El Nino for the theory of its occurrence is still not totally understood. Besides, many signs lack observational sequences. As a result, quantitative predictive models fail to be established. In this study, by using the nonlinear mapping method, the summer EU, WP and WA teleconnection pattern intensity indices combined with May and August SOIs, altogether five variables, are mapped into the two–dimensional space.

Suppose that the observational time is N ($N=40$), the number of variables is M ($M=5$), the distance between samples p and q in the M–dimensional space is d^*_{pq}, and the distance after being mapped into the two–dimensional space is d_{pq}. The target function is defined as

$$K=\frac{1}{\sum\limits_{p<q}^{N} d_{pq}^{*}} \sum_{p<q}^{N} \frac{(d_{pq}^{*}-d_{pq})^{2}}{d_{pq}^{*}}. \tag{1}$$

The nonlinear mapping is the location of the adjusted p and q in the two–dimensional space, enabling all the samples to have $K=\min$.

As

$$d_{pq}^{*}=\sqrt{\sum_{i=1}^{5}(x_{ip}-x_{iq})^{2}}, \quad (p,q=1,2,\cdots,N) \tag{2}$$

$$d_{pq}=\sqrt{(y_{1p}-y_{1q})^{2}+(y_{2p}-y_{2q})^{2}}, \quad (p,q=1,2,\cdots,N) \tag{3}$$

by substituting (2) and (3) into (1) and using the relax method, we have (y_{1p}, y_{1q}), (y_{2p}, y_{2q}), p, $q=1,2,\cdots, N$.

In the y_1, y_2 coordinate, N points are dotted as shown in Fig. 4, in which the anti–El Nino years fall in the fourth quadrant and the El Nino years in the second and third quadrants, showing a very good effect in diagnosing El Nino and anti–El Nino events. Diagnosis by this method shows that the year of 1991 is a new El Nino year.

VI. CONCLUSION

(1) Forty years of monthly and seasonal intensity indices of the five northern teleconnection patterns are calculated by using the northern 500 hPa atmospheric activity center data. Analysis shows that their climatic and lag correlation characteristics both have significant seasonal variations.

(2) The remote response of the winter northern atmospheric circulation to the equatorial Pacific heating field should be the weak WP, and the strong PNA the next. In all the four seasons, the weak WP pattern is an important feature of the circulation when El Nino is at its mature stage. The strong PNA is not necessarily the phenomenon occurring when El Nino is vigorous. In the 1991 / 1992 El Nino event the weak WP rather than the strong PNA pattern occurred.

(3) During the occurrence and development of El Nino, the atmospheric circulation shows anomalies, mainly the strong EU, weak WP and weak WA patterns occurring.

(4) In terms of the three summer teleconnection pattern indices and May and August SOIs, a two–dimensional nonlinear mapping diagram is established so that the El Nino phenomena can be well diagnosed.

REFERENCES

Cao Hongxing et al. (1979), The dimension descending method of multiple–predictor synthesis— — application of nonlinear mapping to weather forecasting, *Sci. Atmos. Sin.*, **3:** 158—165 (in Chinese).

Fennessy, M. J., Marx, L. and Shukla, J. (1985), General circulation model sensitivity to 1982—1983 equatorial Pacific sea surface temperature anomalies, *Mon. Wea. Rev.*, **113:** 858—864.

Horel, J. O. and Wallace, J. M. (1981), Planetary scale atmospheric phenomena associated with the Southern Oscillation, *Mon. Wea. Rev.*, **109:** 813—829.

Hoskins B. J. (1981), Dynamical processes in the atmosphere and the use of models, *Quart. J. Roy. Meteor. Soc.*, **109:** 1—21.

Hoskins, B. J. and Karoly, D. J. (1981), The steady linear response of a spheric atmosphere to thermal and orographic forcing, *J. Atmos. Sci.*, **38:** 1178—1196.

Huang Ronghui (1986), Physical mechanism of influence of heat source anomaly over low latitudes on general circulation over the Northern Hemisphere in winter, *Scientia Sinica (Series B)*, **1:** 91—103.

Huang Ronghui (1991), Role of basic flow in the influence of ENSO on winter circulation over the Northern Hemisphere, *Sci. Atmos. Sin.*, **15:** 44—55 (in Chinese).

Quinn, W. H. et al. (1978), Historical trends and statistics of the Southern Oscillation, El Nino, and Indonesian droughts, *Fishery Bulletin*, **76:** 663—678.

Shi Neng (1989), The multiple statistical analysis of the SOI and its relation to the NH 500 hPa monthly mean circulation, *Acta Meteorologica Sinica*, **47:** 457—465 (in Chinese).

Shi Neng and Luo Boliang (1991), Teleconnection of the 500 hPa polar circulation and El Nino / SO with the temperature field in China, *Adv. Atmos. Sci.*, **8:** 289—298.

Shukla, J. and Wallace, J. M. (1983), Numerical simulation of the atmospheric response to equatorial sea surface temperature anomalies, *J. Atmos. Sci.*, **40:** 1613—1630.

Wallace, J. M. and Gutzler, D. S. (1981), Teleconnections in the geopotential height field in the Northern Hemisphere, *Mon. Wea. Rev.*, **109:** 784—812.